

Electroless Plating on Porous Carbon Felts in Redox Flow Batteries and Thickness Effect on the Electrical and Mechanical Properties

Yiin-Kuen Fuh^{1,*}, Tien-Chan Chang² and Jun-Pu Zhang¹

¹ Department of Mechanical Engineering, National Central University, No.300, Jhongda Rd., Jhongli City, Taoyuan County 32001, Taiwan (R.O.C.)

² Institute of Nuclear Energy Research, Atomic Energy Council, Executive Yuan, No. 1000, Wenhua Rd., Jiaan Village, Longtan Township, Taoyuan County 32546, Taiwan (R.O.C.)

*E-mail: mikefuh@ncu.edu.tw

Received: 18 April 2013 / *Accepted:* 5 June 2013 / *Published:* 1 July 2013

Redox-flow batteries, in particular vanadium redox flow battery (VRB), are receiving intensive attention due to their ability to store large amounts of electrical energy in a relatively cheap and efficient scenario. One of the key components in VRB is carbon felt, which serves as the liquid diffusion layers (LDL) and differentiates distinctively from the gas diffusion layers (GDL) in proton exchange membrane fuel cell (PEMFC) such that the thickness LDL is in mm range, whereas GDL is only 1/5 – 1/10 of it. One reason for a significantly thick carbon felt is due to the enhancement of diffusion length for the VRB while the associated resistance should be minimized. While the thickness of LDL plays the role of stress absorber and maintains the conductivity and the electrical contacts, the durability of the MEA is reasonably safeguarded. This paper adopts a new Ni plating carbon felt and the effect of plating thickness on mechanical, electrical and morphological properties are also discussed. Experimental results show that the nickel coated carbon felt prepared by electroless plating was successfully applied and a drastically reduced ASR of 50% can be obtained under 40% compression, while the stress-strain curve, residual strain and porosity basically remain unchanged. The nickel coated carbon felt is a promising electrode material for VRB application.

Keywords: Vanadium redox flow battery (VRB); Carbon felt; electroless plating

1. INTRODUCTION

A continuously increasing interest in energy storage for the grid and remote power systems is predominantly prevailing in the world due to multiple causes such as the capital costs of managing

peak demands, the grid reliability investments and the integration of renewable energy sources [1]. Among the energy storage methods, redox-flow batteries originating in the 1960s are enjoying much attention due to their ability to store large amounts of electrical energy relatively cheap and efficient. In particular, the all-vanadium (1.26 V) system is one of the most advanced and has reached the demonstration stage for stationary energy storage due to flexible design, long life, and low-cost maintenance [2]. The key components of the vanadium redox flow battery (VRB) can be classified into frame, electrode, ion exchange membrane, current collector (bipolar), pump, storage tank and relevant modeling techniques have been developed [3]. Recent reviews on the Redox Flow Batteries (RFBs) and the underlying physical processes such as various transport and kinetic phenomena were investigated [4].

Due to the relatively recent progress of VRB as the promising energy storage devices, especially for the renewable energy such as solar and wind power, the fundamental knowledge of the liquid diffusion layers (LDL) is still missing, whereas it is essential to have a solid knowledge and relation between the current bipolar plates and active layers [5]. To the best knowledge of the authors, direct measurements of the influence of compression on MEA performances have only been performed using GDL, not the carbon felts as LDL in RFBs [6]. Nevertheless, the correlation between fuel cell performances with the GDL properties is difficult to obtain since the latter are not known. This phenomenon is clarified by a more detailed study that the mass transfer losses increase with the clamping force, irrespective of woven or non-woven gas diffusion backings [7]. Furthermore, the electrical contact resistance is found to be highly influenced by both the clamping force [8]. Least but not the last, the durability of the MEAs, includes GDL, plays an important role as a point of major concern for the end users [9]. The compression and deformation of the carbon felt depends on many parameters, such as the elastic modulus and thickness, clamping force, the pressures of the redox electrolyte flows, gasket material and thickness, temperature, humidity, etc. The deformation of those materials contributes directly the efficiency of the flow-cell assembly and stack. If the clamping force is unreasonably small or large, the system efficiency is reduced and an optimal region has been identified experimentally [5-6,10]. After being clamped together in a fuel cell system, the carbon felt serves as GDL or LDL may be one of the components with the most deformation. The change of permeability or the pore size will inevitably influence greatly the power density or efficiency of the fuel cell system [11–13]

For the metallic coatings on non-metallic substrate, there exists a variety of methods such as chemical vapor deposition (CVD), physical vapor deposition (PVD), electroless plating and thermal spraying. Electroless plating is considered as one of the extensively used and commercially available methods. In particular, the ability to deposit various materials with different sizes and irregular shapes without applied current demonstrates the key strength [14]. For a wide range of material systems and substrates applicable to the electroless plating, recent efforts include silver nanoparticles deposition on porous silicon [15], PdNiCP metallic glass films on pure Cu and pure Al substrates [16], Co coated carbon felt (Co-CF) [17] and nickel–iron and nickel–iron–phosphorus nanomodified Ni-carbon felt anodes [18-19]. In addition, previous researches showed that the modifications of carbon felts using various metallic inclusions such as Mn(IV), Fe(III), Pt, tungsten carbide, polyaniline/Pt composites can improve electrocatalytic activity and the anode performance [20–21]. Furthermore, the unfavorably

formation of passive surface film on the steel current collector can be minimized via electroless silver layer in rechargeable alkaline MnO₂-Zn batteries [22]. Accordingly, similar modifications for the corrosion resistance are also widely reported such that electrolessly plated Ni-P/nano-TiO₂ and Ni-P/CNT composite coatings on 5083 aluminum alloy [23], Ni-Fe-P alloys were deposited onto copper substrate [24] and Ni-P coatings on aluminum foams [25].

This paper has been focused on feasibility study of electroless plating on porous structure of carbon felts and the associated plating thickness effect. Mechanical, morphological and electrical measurements have been systematically conducted to investigate the effectiveness of plating. The in-house measuring device has been used to characterize the through-plane electrical resistance of the LDLs under compression such that the strain–stress curves have been recorded to compare their compressive behavior (percentage of compression versus applied compressive stress from 0 to 4MPa). For the porosity measurement, a pycnometer method is used to compare the porosity of the carbon felts with the electroless plating thickness in the range of 0-1.5 μ m.

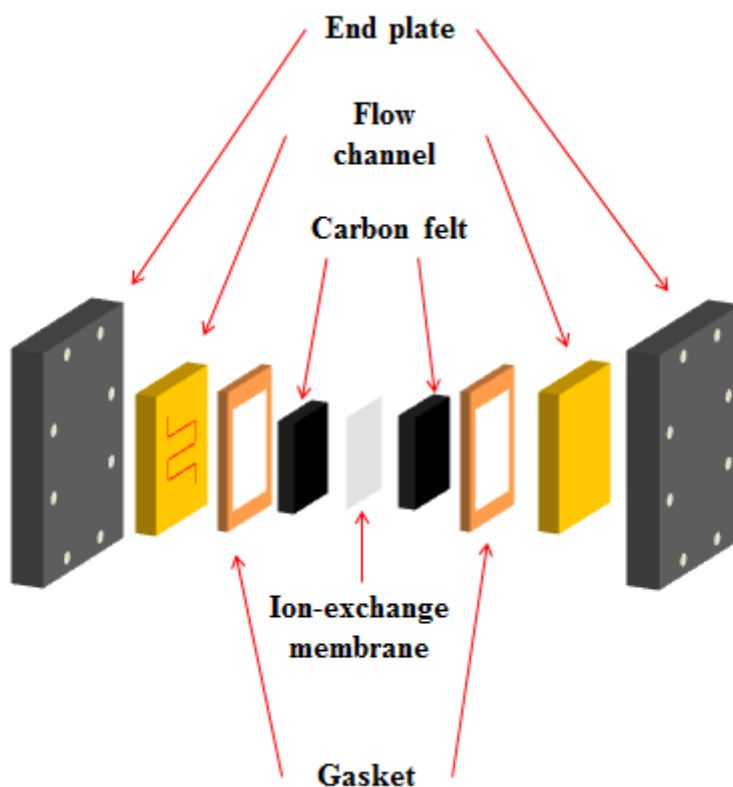


Figure 1. A common VRB unit cell with a significant thickness of carbon felt, typically in the range of 3-5mm thick, primarily functions for compensating the long diffusion length of liquid.

2. CHARACTERIZATION OF CARBON FELTS AND ELECTROLESS PLATING

A common VRB unit cell with a significant thickness of carbon felt can be illustrated in Figure 1. Due to the long diffusion length of liquid used in VRB, a relatively thick carbon felt in the range of 3-5mm are used to compensate this phenomena. Carbon felt plays a complex role in the VRB setup

and its functionalities such as mechanical, electrical and morphological properties are of great concern and importance. In addition, while the thickness of LDL plays the role of stress absorber and maintains the conductivity and the electrical contacts, the durability of the MEA is reasonably safeguarded. Previous studies showed that initial strain due to compression can greatly minimize the contact resistance. On the other hand, the porosity for enhancing the mass transport is also reduced [8]. In this study, we apply another strategy for reducing the contact resistance by using electroless plating technique on the carbon felt, the effects of plating thickness and relevant impact on the mechanical, electrical and morphological properties is investigated.

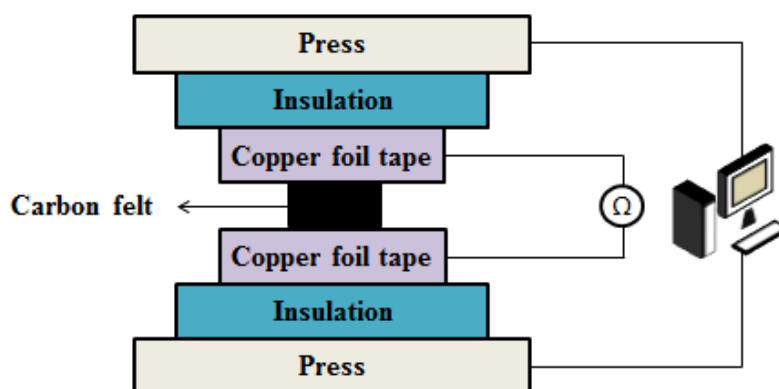


Figure 2. Schematic of the experimental setup for concurrently measuring the mechanical properties of stress-strain and contact resistance under different percentage of compression. Conductive copper foil tape is used for the contact resistance measurement.

2.1. Experimental setup



Figure 3. Electroless plating setup for the electroless plating of Ni (a) degreasing (b) acid cleaning (c) neutralizing with alkaline (d) electroless plating of Ni (e) ultrasonic cleaning (f) water cleaning and rinsing

The mechanical and electrical measurements have been performed with an HT 9102 Floor Standing (Hungta, Taiwan) mechanical bench with a 100kN cell. A four-point resistance measurements device is included while two copper foil tape for maintaining the samples. Each sample records the percentage of compression measured versus the compressive stress in the range 0–4MPa. Two successive compressions at 1 and 4MPa have been applied on each sample: the first one of 1 MPa compares with the pressing commonly used to make the membrane electrodes assemblies and the second one of 4MPa shows the possible crushing or compression caused by the bipolar plates. The resistance measurements have been done simultaneously such that the only results available for the moment represent the addition of the bulk resistance of the carbon felt sample and the two contact resistances between the samples and the copper foil tapes.

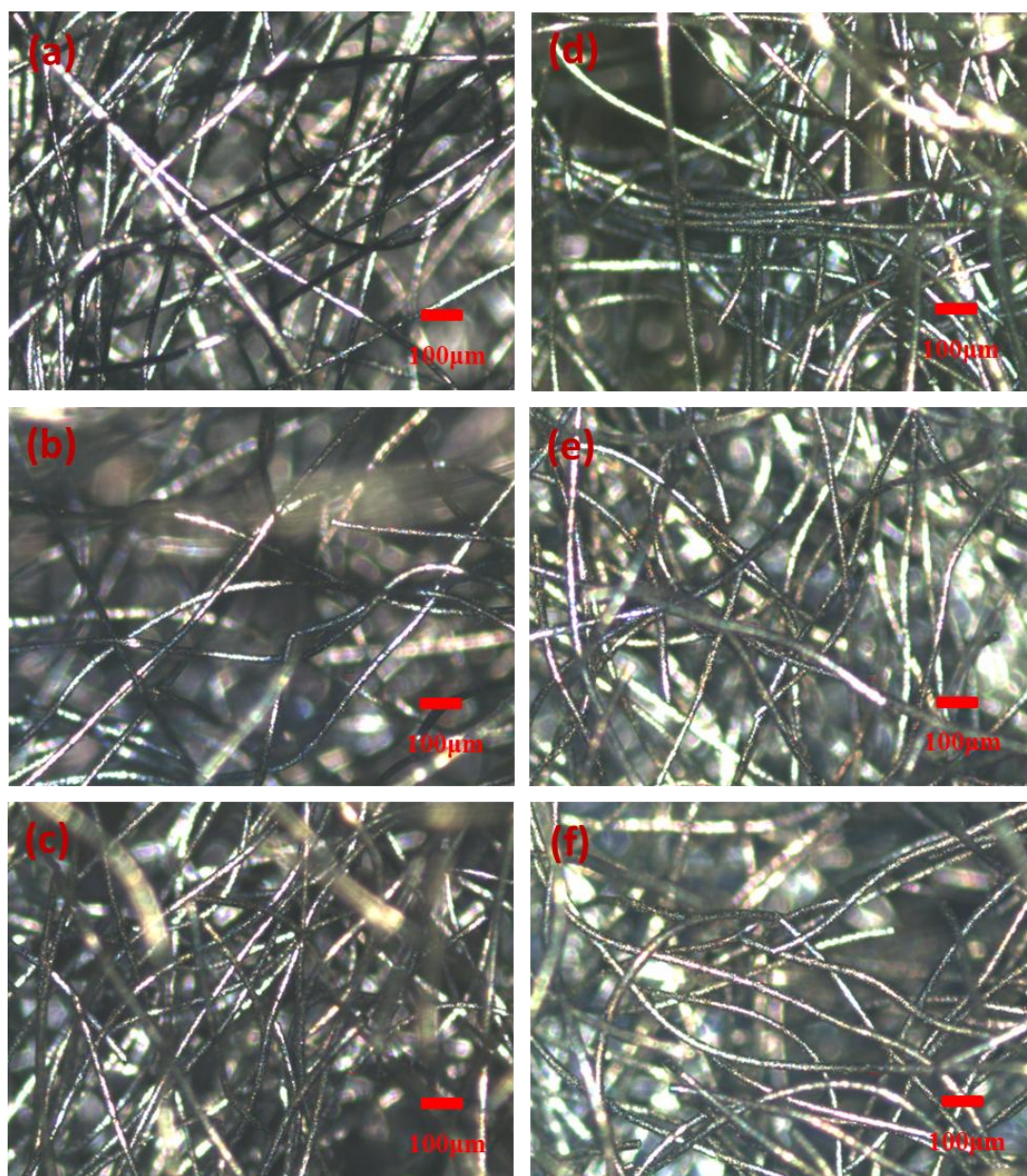


Figure 4. Micrographs (Optical microscope (OM)) of the original carbon felt in (a) and various plating thickness of (b) 0.1 (c) 0.3 (d) 0.5 (e) 1 (f) 1.5µm, respectively.

For the porosity measurement, a pycnometer method is used to compare the porosity of the carbon felts with the electroless plating thickness in the range of 0-1.5 μm .

The experiments for electroless plating of Ni are carried out in a commercial plating company (Tien Co., Taiwan) and the process layout can be shown in Figure 3. For a typical procedure, the carbon felts (Hephas, Taiwan) should submit to the material analysis to check the composition and possible cross-contamination. The following treatments can be classified as the following modules: (I) degreasing (II) removing of any impurity such as oxides (III) acid cleaning (IV) activation of electrolyte (V) introducing into an electroless plating bath. The composition of the plating solution are nickel 92~94% and phosphorous 6~8%. During plating, the bath was maintained at a temperature of 93°C \pm 1°C via a constant temperature regulator. In addition, the pH of the bath is also maintained at constant 4.5 during the plating process.

2.2. Sample description

The electroless plating experiments have been conducted on carbon felt and various plating thickness in the range of 0.1-1.5 μm are shown in Figure 4 (a)-(f). The carbon felts are commercially available and supplied by Hephas Co. The Hephas (100W) carbon felts, widely used in the VRB industry and the customers ranging from Taipower to Institute of Nuclear Energy Research (INER). Figure 4 shows the optical photos taken by optical microscope (OM) for the original carbon felt and various Ni-plating thicknesses. The dimension of carbon felt for the plating experiment is 10mm \times 10mm \times 5mm (length \times width \times thick) and the plating thickness is obtained by using the dummy sample of the same materials with a flat surface. As the plating thickness increases, the carbon fibers are plated with Ni progressively from the outer surface. For the plating thickness of 1 μm and above, the metallic color of Ni can be discernible and no black color of carbon fibers can be seen. It is noticed that the uniformity of plating thickness for porous material is inferior to the flat sample and the effect on electrical, mechanical properties will be discussed in later material characterization.

3. RESULT AND DISCUSSION

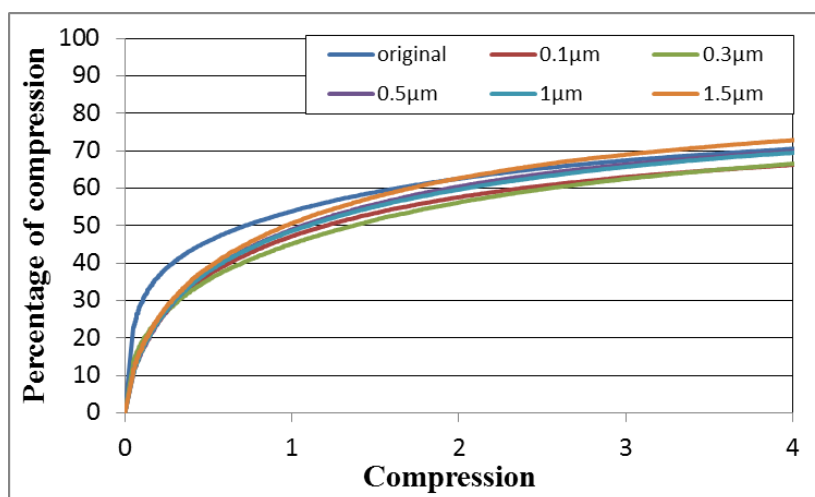


Figure 5. Percentage of compression vs. Compression for original and plating carbon felt.

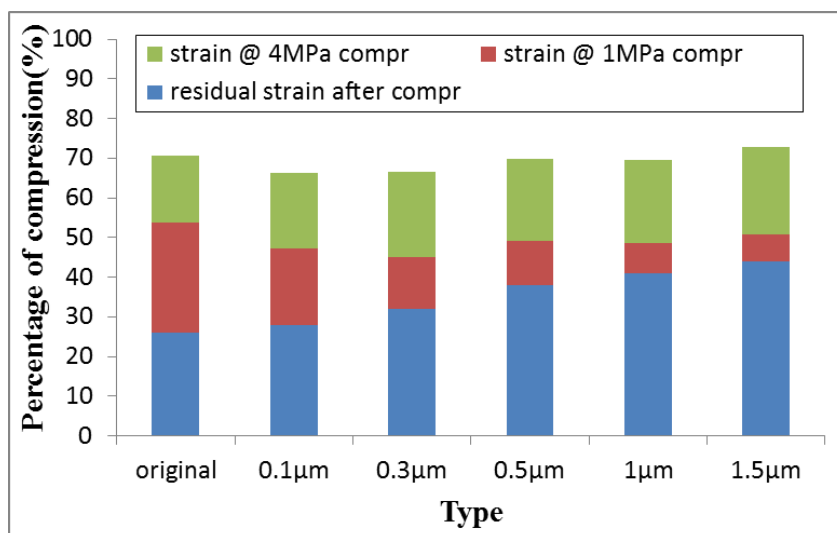


Figure 6. Compressive strain and residual strain observed for original and plating carbon felt after the compression test.

3.1. Mechanical results

The carbon felts with various plating thickness present strikingly similar compressive behaviors as shown in Figure 5. Noticeably, two different behaviors at low and high compressive stress are existed during the first compression with a large slope of compressive strain which decreases strongly after 1MPa. It is reasonable that original carbon felt shows higher compression ratio under the same compression force while the plating Ni will decrease the compression strain due to extra stiffness of plated Ni. However, for the plating thickness in the range of 0.1-1.5µm, the mechanical property of stress-strain curve shows the similar trend, both quantitatively and qualitatively. Negligible difference is observed due to initial strain and basically indiscernible for compression under 1MPa.

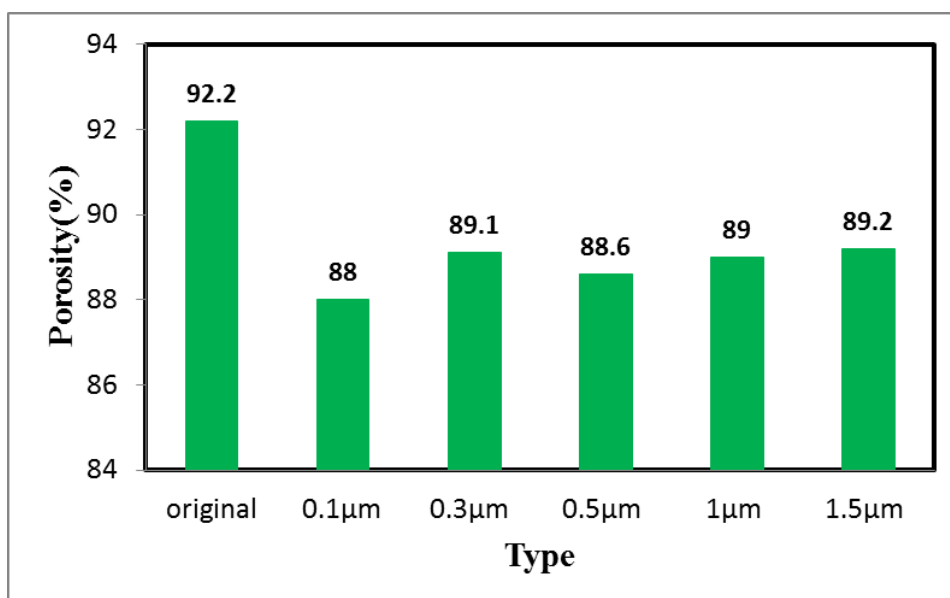


Figure 7. Comparison of porosity obtained by pycnometer method.

The compressive strain at two levels of pressure and the residual strain, during and after the first cycle can be extracted from the experimental data, respectively in Figure 6. As expected, the extra thickness of electroless plating Ni will inevitably increase the stiffness. The level of residual strain after the first compression is the highest for the sample of 1.5 μm thick and the value is almost 1.6 times higher as compared to the original sample without electroless plating (44% v.s. 26%). During the second compression, all samples exhibit similar total strain in the range of 66-72% at 4MPa. Therefore, this indicates that the extra Ni thickness as high as 1.5 μm will not significantly hamper the balance of compressive stress, despite in different compression at 1 and 4 MPa respectively, total mechanical compression behavior remain similar to the original sample. This experiment demonstrates that electroless plating of 1.5 μm will have minimal impact on the contact resistance if suitable stress of 4MPa persists.

3.2. Porosity characterization under various percentage of compression

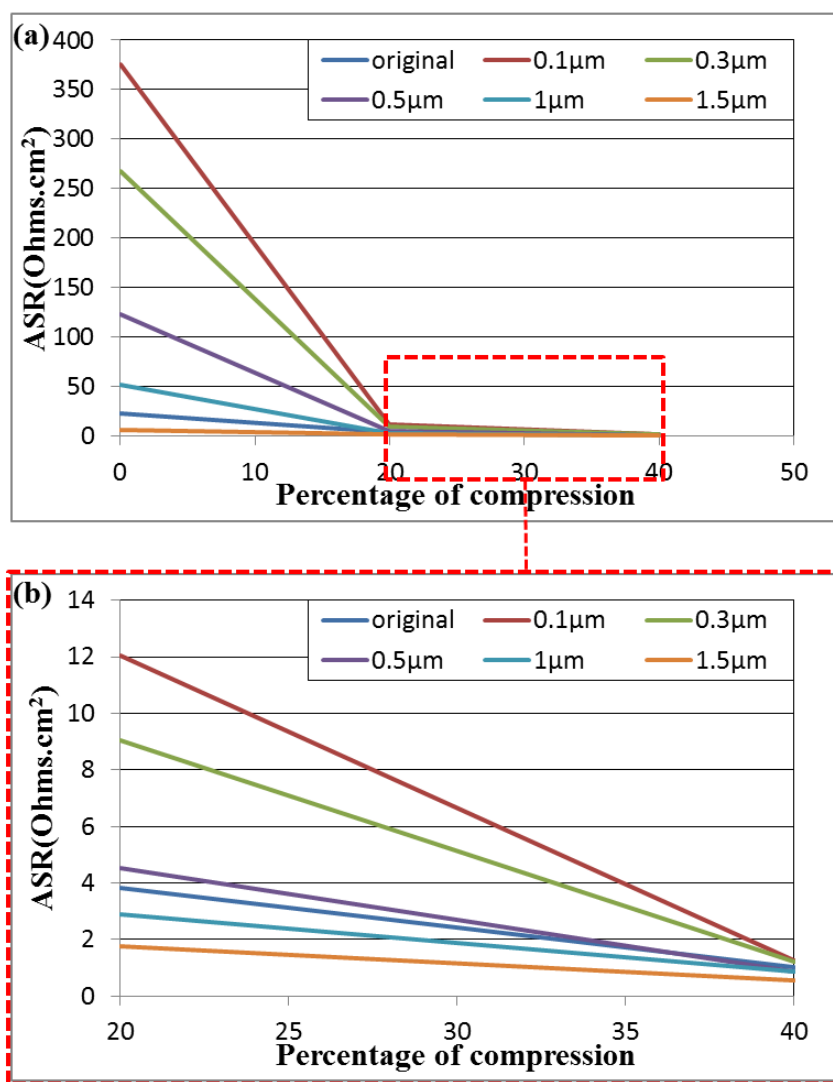


Figure 8. (a)ASR vs. Percentage of compression for original and plating carbon felt (b) Enlargement of compression between 20-40%.

The porosity measurement by pycnometer method for the selected samples is shown in Figure 7. The results indicate that porosity distribution is in the range of 88-92% and the specific porosity for the 0, 0.1, 0.3, 0.5, 1, 1.5 μm are 92.2%, 88%, 89.1%, 88.6%, 89% and 89.2%, respectively. This result clearly shows that the extra plating process has a very minimal effect of the porosity and the overall reduction in porosity is less than 4%.

Table 1. Original and plating carbon felt resistance under different percentage of compression

Type	ASR (Ωcm^{-2}) for 0% compression	ASR (Ωcm^{-2}) for 20% compression	ASR (Ωcm^{-2}) for 40% compression
original	22.94	3.84	1.02
0.1 μm	375.3	12.05	1.25
0.3 μm	267.5	9.04	1.21
0.5 μm	122.5	4.52	0.87
1 μm	51.4	2.88	0.86
1.5 μm	6.32	1.78	0.54

3.3. Electrical part-interfacial contact resistance

In order to obtain more accurate results of mechanical compression on electrical properties, conductivity measurements have been performed. It is noted that the measured electrical resistance is a combination of one bulk resistance and two contact resistances between the surfaces of the sample and of the copper foils as shown in Figure 2. It is experimentally measured that electrical resistance decreases quickly with the stress applied for all samples up to 20% compression and followed by a relatively gradual decrease as shown in Figure 8. It can mainly be ascribed to the abrupt decrease of contact resistances due to the effect of mechanical compression. Specifically, at the percentage of compression 20%, the bulk resistances for samples of electroless plating 0, 0.1, 0.3, 0.5, 1, 1.5 μm thick are measured as 3.84 $\Omega\text{-cm}^2$, 12.05 $\Omega\text{-cm}^2$, 9.04 $\Omega\text{-cm}^2$, 4.52 $\Omega\text{-cm}^2$, 2.88 $\Omega\text{-cm}^2$, 1.78 $\Omega\text{-cm}^2$. At the percentage of compression 40%, the measured resistances are 1.02 $\Omega\text{-cm}^2$, 1.25 $\Omega\text{-cm}^2$, 1.21 $\Omega\text{-cm}^2$, 0.87 $\Omega\text{-cm}^2$, 0.86 $\Omega\text{-cm}^2$, 0.54 $\Omega\text{-cm}^2$, respectively, as shown in the inset of Figure 8 (b). It is observed that for samples smaller than 1 μm thick exhibit even higher ASR as compared to the original sample. The possible reason may be attributed to the cross contamination of industrial equipment used such that the initial plating thickness is not pure Ni. Another possibility is the porous nature of carbon felt, which makes the plating process even more challenging. However, for the samples of 0 and 1.5 μm thick, ASR measured to be 3.84 $\Omega\text{-cm}^2$ 1.78 $\Omega\text{-cm}^2$ for 20% compression and 1.02 $\Omega\text{-cm}^2$ 0.54 $\Omega\text{-cm}^2$ for 40% compression, respectively. The reduction of ASR is effectively achieved by 50% due to the extra 1.5 μm thick Ni. Table 1 lists the numerical values of measured ASR values.

4. CONCLUSION

In this paper, the successful deposition of Ni on porous carbon felts is demonstrated and associated properties such as mechanical compression on the electrical conductivity and porosity are

characterized. From the OM observation, the uniformity and integrity of plating Ni for various thickness is demonstrated. For the samples of 1.5 μ m plating thickness, measurement result shows a significantly reduced ASR of 50% for 40% compression, while the stress-strain curve, residual strain and porosity basically remain unchanged. This shows the effectiveness of carbon felt modification via Ni electroless plating and can be a promising tool to further enhance the efficiency of the flow batteries. The future work will apply these plating carbon felts to the actual VRB and investigate the relation of enhanced conductivity and the electrical contacts as well as VRB performance.

ACKNOWLEDGEMENTS

We gratefully acknowledge the financial support by the National Science Council of Taiwan under contract No.: NSC 101-2622-E-008-013-CC3.

References

1. Electrical energy storage technology options (Report 1020676, Electric Power Research Institute, Palo Alto, CA, December(2010).
2. B. Dunn, H. Kamath, J.M. Tarascon, *Science* 334, 928 (2011).
3. D. Youa, H. Zhanga, J. Chena, *Electrochim Acta* 54 (2009) 6827–6836.
4. M. Skyllas-Kazacos, M. H. Chakrabarti, S. A. Hajimolana, F. S. Mjalli, M. Saleemd, J. *Electrochem*, 158 (8) R55–R79 (2011).
5. F. Mishra, F. Yang, R. Pitchumani, *J. Fuel Cell Sci. Technol.* 1 (2004) 2–9.
6. W.K. Lee, C.H. Ho, J.W.V. Zee, M. Murthy, *J. Power Sources* 84 (1999) 45–51.
7. J. Itonen, M. Mikkola, G. Lindbergh, *J. Electrochem, Soc.* 151 (2004) A1152–A1161.
8. P. Zhou, C.W. Wu, G.J. Ma, *J. Power Sources* 159 (2006) 1115–1122.
9. S. Escribano, J. F. Blachot, J. Eth`eve, A. Morin, R. Mosdale, *J. Power Sources* 156 (2006) 8–13.
10. H. Wang, M.A. Sweikart, J.A. Turner, *J. Power Sources* 115 (2003) 243–251.
11. J. Soler, E. Hontanon, L. Daza, *J. Power Sources* 118 (2003) 172–178.
12. M. Prasanna, H.Y. Ha, E.A. Cho, et al., *J. Power Sources* 131 (2004) 147–154.
13. J.G. Pharoah, *J. Power Sources* 144 (2005) 77–82.
14. K.L. Yung, Y. Xu, C.L. Kang, B. Q. Jiang, *Journal of Materials Processing Technology* 213 (2013) 136–142.
15. H. Yan, N. Xu, W. Y. Huang, H. M. Han, S. J. Xiao, *International Journal of Mass Spectrometry* 281 (2009) 1–7.
16. A. Shibata, Y. Imamura, M. Sone, C. Ishiyama, Y. Higo, *Thin Solid Films* 517 (2009) 1935–1938.
17. H. Zhou, H. Zhang, P. Zhao, B. Yi, *Electrochemistry* 74 (2006) 296–298.
18. Y. Hubenova, M. Mitov, *Bioelectroch* (2010) 78–57.
19. Y. Hubenova, R. Rashkov, V. Buchvarov, S. Babanova, M. Mitov, *J Mater Sci* 46 (2011) 7074–7081.
20. B.E. Logan, B. Hamelers, R. Rozendal, U. Schro`der, J. Keller, S. Freguia, P. Aelterman, W. Verstraete, K. Rabaey, *Environm Sci Technol* 40 (2006) 5181.
21. A. Rinaldi, B. Mecheri, V. Garavaglia, S. Licocchia, P. Nardo, E. Traversa, *Energy Environ Sci* 1 (2008) 417.
22. M. Ghaemi, F. Makhlooghi, H. Adelkhani, M. Aghazadeh, H. M. Shiri, *Int. J. Electrochem. Sci.* 5 (2010) 131–146.
23. C. K. Lee, *Int. J. Electrochem. Sci.* 7 (2012) 12941–12954.
24. G. F. Huang¹, W. Q. Huang, L. L. Wang, B. S. Zou, D. P. Chen, D. Y. Li, J. M. Wei¹, J. H. Zhang, *Int. J. Electrochem. Sci.* 2 (2007) 321–328.

25. J. Liu, X. Zhu, J. Sudagar, F. Gao, P. Feng, *Int. J. Electrochem. Sci.* 7 (2012) 5951–5961.

© 2013 by ESG (www.electrochemsci.org)